



EXPLORING EFFICIENCY AND DESIGN OPTIMIZATION OF FLEXIBLE PEROVSKITE SOLAR CELLS USING SCAPS-1D SIMULATION

Elif DAMGACI^{1*} , Emre KARTAL² , Ayşe SEYHAN³ 

^{1,2,3} Nigde Omer Halisdemir University, Nanotechnology Research Center, 51240, Nigde, Türkiye
¹ Nigde Omer Halisdemir University, Department of Mechanical Engineering, 51240, Nigde, Türkiye
^{2,3} Nigde Omer Halisdemir University, Department of Physics, 51240, Nigde, Türkiye

ABSTRACT

This research focuses on using SCAPS-1D software to design and simulate efficient flexible perovskite solar cells. The study aims to optimize design parameters, gain a deeper understanding of the underlying physics, and obtain valuable insights into electrical characteristics. The device architecture includes key components like PET/ITO substrate, TiO₂ ETL, CH₃NH₃SnI₃ absorber, CuSCN HTL, and Au electrode. By optimizing the absorber thickness (600 nm) and temperature (300 K), the performance and efficiency of the cell were improved. Investigation of different doping concentrations at 300 K for a fixed thickness revealed an efficiency of 26.98% at 600 nm. The highest efficiency of 31.44% was achieved with a doping concentration of 1E+21. This research showcases the potential of flexible perovskite solar cells for lightweight and versatile applications, emphasizing their significance in the field.

Keywords: Flexible perovskite solar cells, SCAPS-1D, Simulation, Doping, Efficiency.

1. INTRODUCTION

The advent of flexible perovskite solar cells has brought about a promising technology in the realm of photovoltaics. These devices exhibit remarkable power conversion efficiency and possess the unique ability to conform to diverse surfaces. In comparison to traditional rigid solar cells, flexible perovskite solar cells (FPSCs) offer substantial advantages, including their lightweight nature and bendable characteristics. These attributes enable their application in areas where conventional solar cells are impractical or constrained by their rigidity.

The efficiency of FPSCs demonstrated remarkable progress, experiencing a substantial increase from 2.6% to 19.5% over the period of 2013 to 2019. This significant improvement in productivity highlights the rapid advancements in FPSC technology during that timeframe [1,2]. Presently, single-junction FPSCs have achieved power conversion efficiencies (PCEs) of 21.76%. In comparison, tandem-inverted FPSCs have achieved even higher PCEs of 24.7%. These significant efficiency values underscore the promising commercial potential of both single-junction and tandem-inverted FPSCs [3]. The optical and electrical properties of flexible substrate perovskite solar cells produced in different structures with high efficiency over time are given in Table 1.

Table 1. 2013-2023 Flexible perovskite cell efficiency values.

| Configuration | Voc | FF | Jsc | PCE | Ref | Year |
|--|-------|-------|-------|-------|------|------|
| PET/ITO/PEDOT:PSS/Perovskite/PCBM/TiO ₂ /Al | 0.88 | 51 | 14.4 | 6.4 | [4] | 2013 |
| PEN/ITO/ MAPbI _{3-x} Cl _x /Spiro-OMeTAD/Ag | 0.95 | 60 | 21.40 | 12.20 | [5] | 2014 |
| PEN/ITO/ZnO/MAPbI ₃ /PTAA/Au | 1.10 | 75 | 18.7 | 15.4 | [6] | 2015 |
| PET/ITO/ZnO/MAPbI ₃ /PTAA/Au | 1.10 | 79 | 19.3 | 16.8 | [7] | 2018 |
| PEN/ITO/SnO ₂ /Perovskite/Spiro-OMeTAD/Au | 1.08 | 74.9 | 21.3 | 17.3 | [8] | 2019 |
| PEN/ITO/SnO ₂ -CPTA/Perovskite/Spiro-OMeTAD /Au | 1.08 | 75.0 | 22.4 | 18.3 | [9] | 2019 |
| PET/ITO/SnO ₂ NPs/(FAPbI ₃) _{0.95} (MAPbBr ₃) _{0.05} /spiro-OMeTAD/Au | 1.14 | 75.5 | 22.1 | 19.1 | [10] | 2020 |
| PET/PEDOT:PSS/PTAA/Perovskite/PCBM/BCP/Ag | - | - | - | 21.02 | [11] | 2022 |
| PEN/ITO/SAM/PVK/PCBM/BCP/Ag | 1.178 | 83.55 | 23.36 | 23.01 | [12] | 2023 |

* Corresponding author, e-mail: elifdamgaci@gmail.com (E. Damgaci)

Received: 26.05.2023 Accepted: 16.06.2023

doi: 10.55696/ejset.1303146

EXPLORING EFFICIENCY AND DESIGN OPTIMIZATION OF FLEXIBLE PEROVSKITE SOLAR CELLS USING SCAPS-1D SIMULATION

The experimental investigation and characterization of the layers comprising the cell structure have been extensively conducted by numerous researchers, as presented in Table 1. The SCAPS software is utilized to simulate and analyze the performance characteristics of the FPSC device, allowing for the optimization and understanding of its electrical behavior. Using the SCAPS software, a detailed understanding of the device's performance has been gained, contributing to the optimization and advancement of flexible perovskite solar cell technology. Based on these research studies, the simulation program enables the calculation of the cell's efficiency, occupancy factor, current, and voltage values.

2. MATERIAL AND METHOD

SCAPS 1D (Solar Cell Capacitance Simulator) is a powerful software tool widely utilized in the field of solar cell research and development. Its primary function is to simulate and model the intricate electrical behavior exhibited by solar cells. This sophisticated tool enables scientists, engineers, and researchers to delve into the intricacies of solar cell operation, ultimately leading to a better understanding of their performance and aiding in the optimization of various solar cell devices.

The basic equations used in SCAPS programming are:

$$\nabla \cdot \epsilon \nabla \phi = -q(p - n + ND + -NA -) \quad (1)$$

$$Jn = Dn \frac{dn}{dx} + \mu_n n \frac{d\phi}{dx}, \quad Jp = Dp \frac{dp}{dx} + \mu_p p \frac{d\phi}{dx} \quad (2)$$

$$\frac{dj_n}{dx} = G - R, \quad \frac{dj_p}{dx} = G - R \quad (3)$$

The current study presents a model and simulation of a typical PSC with five layers, including a conductive Gold (Au) metal electrode, TiO_2 as the electron transport material (ETM) layer, methylammonium tin tri-iodide ($\text{CH}_3\text{NH}_3\text{SnI}_3$) as the perovskite light absorber layer, Copper (I) thiocyanate (CuSCN) as the hole transport material (HTM) layer, and Indium Tin Oxide (ITO)-coated flexible polyethylene terephthalate (PET) as the substrate. The simulated structure and energy band diagram are given in Figure 1(a) and Figure 1. (b).

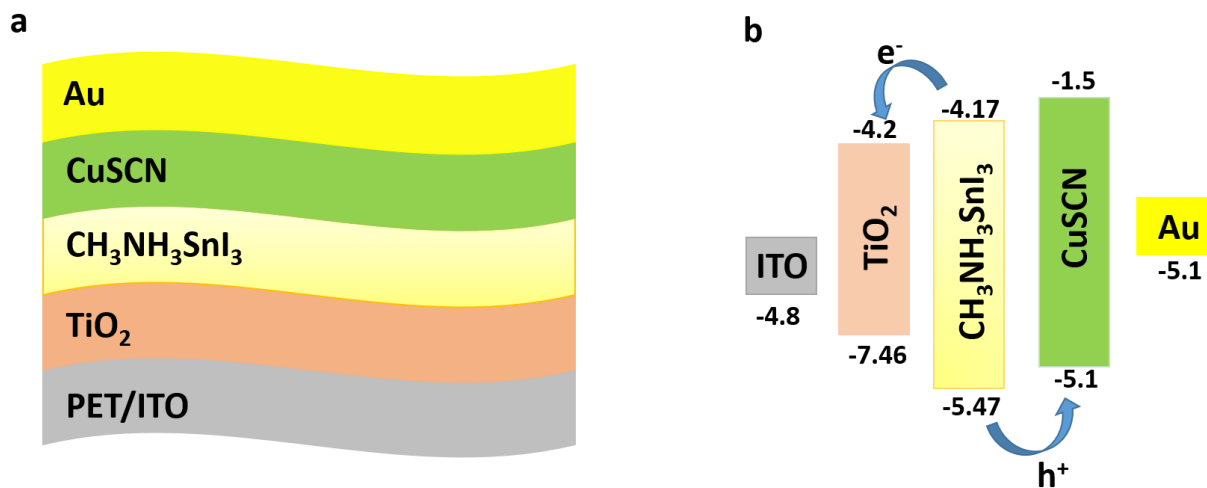


Figure 1. Flexible perovskite solar cell structure (a), the energy band diagram (b).

Burgelman et al. developed and adapted the SCAPS 1D program for the purpose of designing and conducting numerical analysis on the cell architecture of solar cells. The program also enables simulation and numerical analysis of optoelectronic and photovoltaic architectures, providing valuable insights for research in these fields. SCAPS 1D is capable of modeling and analyzing the recombination mechanism, electric field distribution, charge transport, and current densities of various types of

solar cells. It can solve the basic semiconductor equations in one dimension at a steady state, making it suitable for describing the model of any solar cell.

In this study, the most up-to-date version of the program, SCAPS 1D (ver.3.3.10), was used by simulating the device efficiency parameters closest to the literature values. The operation of the program is given in the following steps and the interface shape is shown in Figure 2. SCAPS 1D is a software tool used for simulating and analyzing the performance of photovoltaic devices. Here are the working steps to use SCAPS 1D:

1. Start SCAPS 1D: Launch the SCAPS 1D software on your computer.
2. Set the desired problem: Define the specific problem you want to simulate. This could be the analysis of a specific solar cell structure, material, or device configuration.
3. Input photovoltaic parameters: Provide the necessary input parameters for the simulation. These parameters include material properties, device geometries, doping profiles, and other relevant information specific to the problem you are investigating.
4. Apply the working condition: Specify the working conditions under which you want to analyze the photovoltaic device. This includes setting parameters such as temperature, light intensity, and applied voltages or currents.
5. Run the problem: Initiate the simulation by running the problem within the SCAPS 1D software. The software will use the input parameters and working conditions to calculate the behavior of the photovoltaic device.
6. Analyze the output: After the simulation is complete, SCAPS 1D will provide output data and results. This may include information such as current-voltage characteristics, efficiency, charge carrier distribution, and other relevant performance metrics.

By following these steps, you can utilize SCAPS 1D to simulate and study the behavior of photovoltaic devices under different conditions and configurations [13].

Table 2 presents the essential cell parameters necessary for the simulation, emphasizing their significance. The selection of these values was based on a combination of theoretical analysis, experimental findings, and references from established literature. In certain instances, reasonable approximations were made when data was unavailable [14,15,16]. The majority of absorber layer parameters employed in the simulation were obtained from relevant literature sources.

Table 2. Materials parameters of various layers simulated for flexible perovskite solar cells at A.M. 1.5G.

| Parameter | ITO | TiO ₂ | CH ₃ NH ₃ SnI ₃ | CuSCN |
|--|-----------|------------------|--|-----------|
| Thickness (nm) | 300 | 100 | Varied | 50 |
| Bandgap (eV) | 3.65 | 3.26 | 1.3 | 3.6 |
| Electron affinity (eV) | 4.8 | 4.2 | 4.17 | 1.7 |
| Permittivity (ϵ) | 8.900 | 10 | 6500 | 10000 |
| CB effective DOS (cm ⁻³) | 5.200E+18 | 2.2E+18 | 1.0E+18 | 2.200E+19 |
| VB effective DOS (cm ⁻³) | 1000E+18 | 1.800E+19 | 1.000E+19 | 1.800E+19 |
| Electron thermal Velocity (cm/s) | 2000E+7 | 1.000E+7 | 1.000E+7 | 1.000E+7 |
| Hole thermal Velocity (cm/s) | 1000E+7 | 1.000E+7 | 1.000E+7 | 1.000E+7 |
| Electron mobility, μ_E (cm ² /Vs) | 1000E+1 | 1.000E+2 | 1.600E+0 | 2.500E-1 |
| Hole mobility, μ_H (cm ² /Vs) | 1000E+1 | 2.500E+1 | 1.600E+0 | 2.500E-1 |
| Donor density ND (1/cm ³) | 1000E+20 | 1.000E+19 | 0.00E+0 | 0.00E+0 |
| Acceptor density NA (1/cm ³) | 1000E+15 | 0.00E+0 | Varied | 2.000E+19 |

EXPLORING EFFICIENCY AND DESIGN OPTIMIZATION OF FLEXIBLE PEROVSKITE SOLAR CELLS USING SCAPS-1D SIMULATION

Table 3. The basic material parameters of the back and front contacts for cell.

| Electrical properties @ 300 K | BC (Au) | FC(PET/ITO) |
|--|---------|-------------|
| Thermionic emission/surface recombination velocity of electron(cm/s) | 10^5 | 10^7 |
| Thermionic emission/surface recombination velocity of hole(cm/s) | 10^7 | 10^5 |
| Work function(eV) | 5.1[17] | 4.7[18] |

*BC:Back contact, FC:Front contact

The software interfaces incorporate all the variables listed in Table 2 and Table 3, which serve as input parameters for the device simulation. This ensures that the simulation accurately reflects the behavior of the physical device. Moreover, it provides a comprehensive list of the parameters considered throughout the procedure, enabling the exploration of different elements' effects on device performance by manipulating variables. Figure 2 below illustrates the detailed simulation procedure. This program, which can be applied to various solar cells, is updated with different materials and photovoltaic parameters.

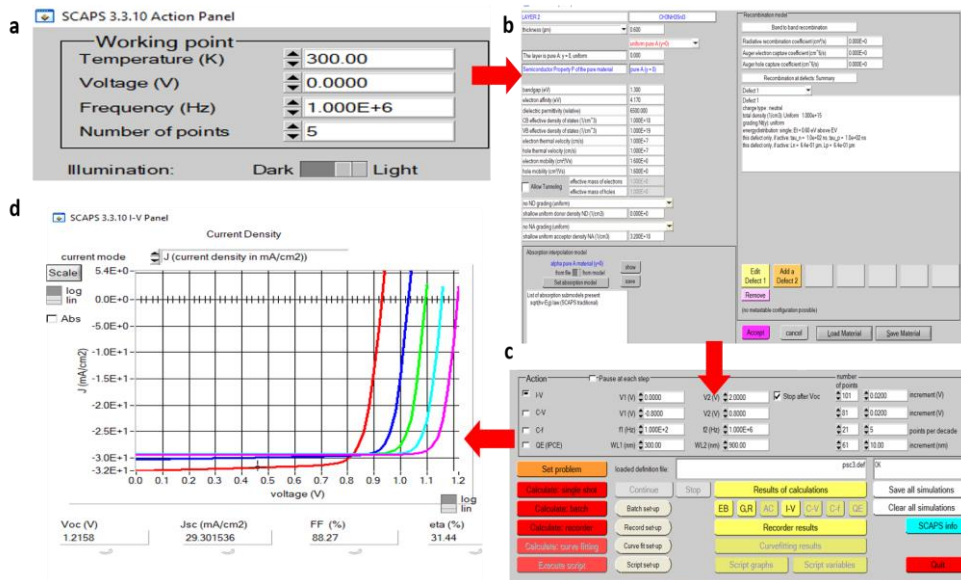


Figure 2. The SCAPS 1D working point (a), setting problem and Input Photovoltaic Parameters (b), batch calculation and record calculation (c), J-V results (d).

3. RESULTS AND DISCUSSION

Overall, understanding and addressing the impact of temperature on flexible perovskite solar cells are crucial for optimizing their performance, stability, and long-term reliability, thereby facilitating their widespread adoption as a renewable energy technology. High temperatures have a detrimental impact on the power conversion efficiency of flexible perovskite solar cells. The underlying cause is the accelerated occurrence of non-radiative recombination processes within the perovskite layer. This elevated recombination rate leads to a drop in both the open circuit voltage and the fill factor, resulting in an overall drop in efficiency. These effects can be observed in figures generated using SCAPS 1D simulations. Table 4 shows detailed simulation data of simulated flexible photovoltaic cells (FPCs) on filling factor (FF), open circuit voltage (Voc), FF, short circuit current density (Jsc), and variable temperature effect on PCE. In Table 5, Simulated FPCs were investigated with varying thicknesses to examine their effects on FF, Voc, Jsc, and PCE. Due to the deformation and increased stress resulting from temperature elevation, the layers within the simulated model may experience enhanced interconnectivity. PET/ITO melting temperature ranges from 120 degrees to 260 degrees. This percentage has been optimized considering the temperature value in the simulation. This can lead to a decrease in fill factor and efficiency, as the rise in series resistance coincides with a reduction in diffusion length [19].

To achieve high efficiency, the optimum temperature for the simulated model was determined to be 300 K, as depicted in figure 3. Furthermore, the thickness optimization procedures were conducted at this temperature.

Table 4. Varies temperature effect on Voc, FF, Jsc, and PCE of the simulated FPSC.

| Temperature (K) | Voc | FF | Jsc | Eta% |
|-----------------|--------|-------|-----------|-------|
| 250 | 1.1159 | 79.93 | 28.69585 | 25.60 |
| 298.15 | 1.0657 | 85.63 | 29.553916 | 26.97 |
| 300 | 1.0636 | 85.74 | 29.579213 | 26.98 |
| 350 | 1.0078 | 85.81 | 30.127254 | 26.06 |
| 400 | 0.9502 | 84.11 | 30.508975 | 24.38 |
| 450 | 0.8906 | 82.11 | 30.803791 | 22.53 |
| 500 | 0.8292 | 79.80 | 31.035678 | 20.54 |

Table 5. Varies thickness effect on Voc, FF, Jsc, and PCE of the simulated FPSC at 300 K.

| Thickness (nm) | Voc | FF | Jsc | Eta% |
|----------------|--------|-------|-----------|-------|
| 400 | 1.0681 | 86.16 | 28.827141 | 26.53 |
| 500 | 1.0656 | 86.00 | 29.411375 | 26.95 |
| 600 | 1.0636 | 85.74 | 29.579213 | 26.98 |
| 700 | 1.0620 | 85.66 | 29.560310 | 26.89 |
| 800 | 1.0607 | 85.60 | 29.467137 | 26.76 |
| 900 | 1.0598 | 85.56 | 29.353818 | 26.62 |
| 1000 | 1.0591 | 85.53 | 29.244978 | 26.49 |

The performance of solar cells is influenced by the thickness of the absorber layer (L). Figure 3 demonstrates how varying the absorber layer thickness impacts performance parameters such as Voc, Jsc, FF, and PCE. In the cells that underwent thickness optimization, the highest efficiency value of 26.98% was achieved at a thickness of 600 nm.

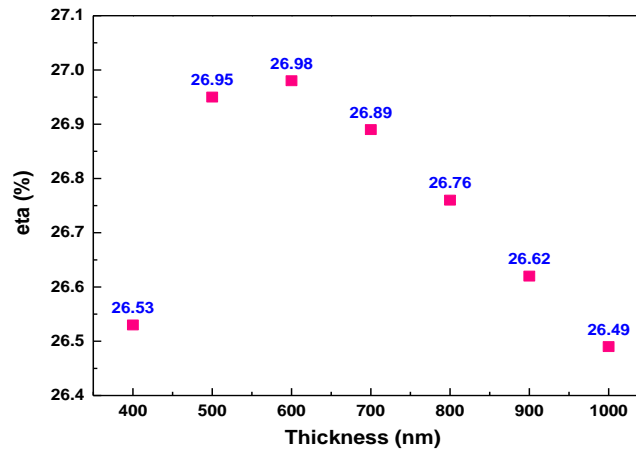


Figure 3. The effect of $\text{CH}_3\text{NH}_3\text{SnI}_3$ layer thickness on efficiency.

In the SCAPS 1D simulation, the acceptor density (NA) is an important parameter that is considered to accurately model the behavior of the device. The concentration of doping within the absorber material significantly impacts the performance of photovoltaic systems. The study examines the performance of a proposed flexible perovskite solar cell by investigating its response to different doping densities in the absorber layer. Figure 4 displays the variations of Voc, Jsc, FF, and overall efficiency of the designed perovskite solar cell as a function of the doping concentration in the absorber layer.

EXPLORING EFFICIENCY AND DESIGN OPTIMIZATION OF FLEXIBLE PEROVSKITE SOLAR CELLS USING SCAPS-1D SIMULATION

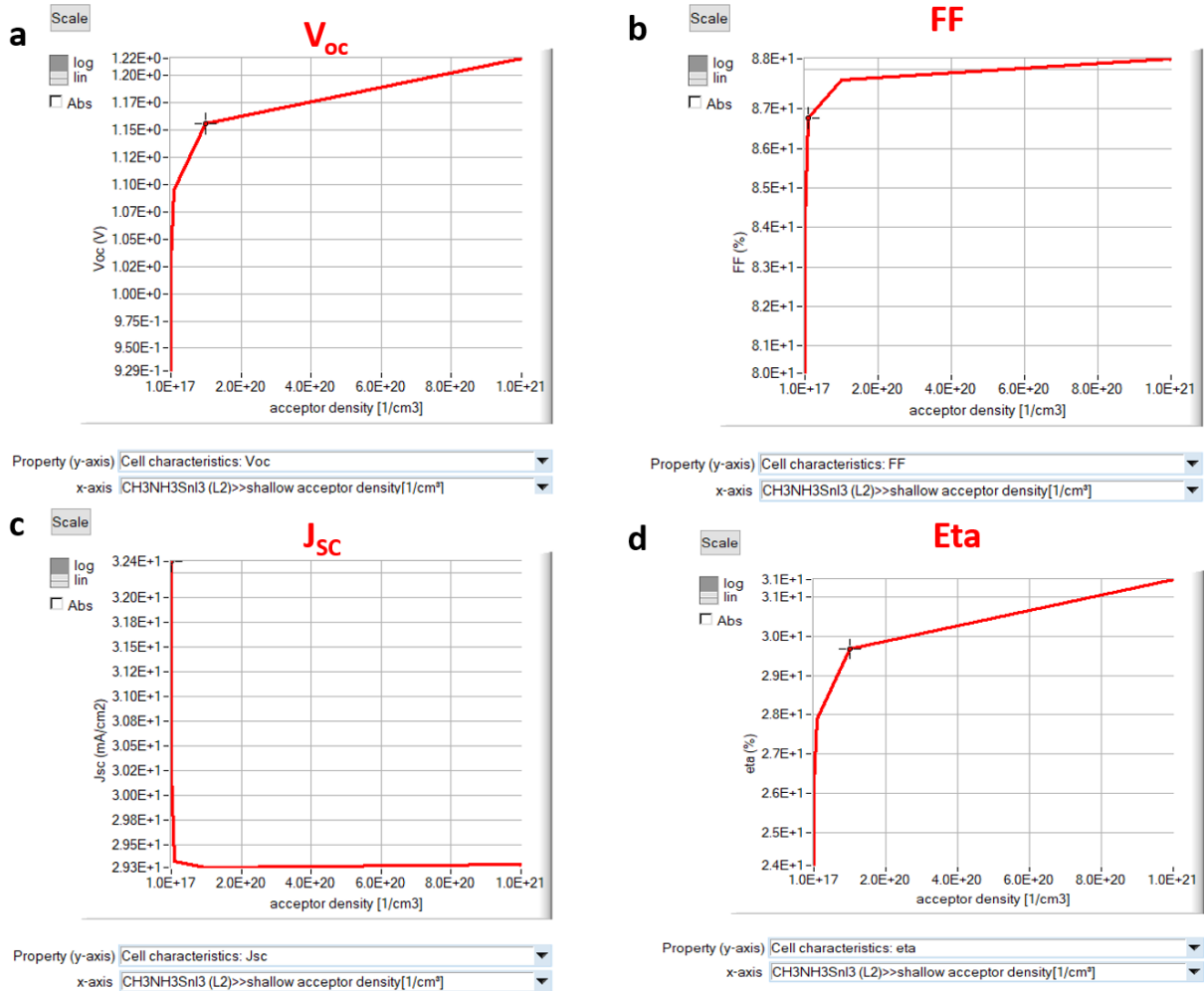


Figure 4. The effect of NA of the CH₃NH₃SnI₃ absorber layer on the performance of (a) Voc, (b) FF (c) Jsc, and (d) PCE.

Shallow uniform acceptor density NA (1/cm³) effect on Voc, Jsc, FF, and efficiency is as follows; firstly, the acceptor doping concentration affects the energy levels and recombination processes in the perovskite layer. An optimal NA can create an appropriate energy gradient, reducing recombination and enhancing the Voc. Secondly, the acceptor doping concentration also influences the charge carrier transport and recombination within the perovskite layer. An optimized NA can enhance charge carrier mobility, minimize recombination losses, and improve the FF. When a solar cell operates at a higher fill factor, it typically operates closer to its maximum power point, which corresponds to the optimal balance between voltage and current. By operating at higher currents and voltages closer to the maximum power point, the overall power conversion efficiency of the solar cell increases. This, in turn, means that a higher fraction of the incident light is being effectively converted into usable electrical power, reducing the potential for parasitic absorption. Thirdly, the acceptor doping concentration indirectly affects the Jsc by influencing the charge carrier generation and transport. In some cases, an appropriate NA can enhance the Jsc by optimizing the charge carrier extraction and reducing recombination. However, if NA is excessively high, it can increase trap-assisted recombination and hinder the charge carrier generation, leading to a decrease in Jsc. Therefore, it is important to carefully select the acceptor doping concentration in the perovskite layer to achieve higher Voc, FF, and Jsc, striking a balance between optimizing charge carrier transport and minimizing recombination losses. In this study, simulating the doping concentration in the range of 1x10¹⁷ to 1x10²¹, it was observed that the Voc and FF increased, while the Jsc decreased. This suggests that there is an optimal doping concentration within this range that enhances Voc and FF but compromises Jsc. It indicates a trade-off between improving Voc and FF while potentially sacrificing Jsc in the context of the specific doping concentrations studied [20].

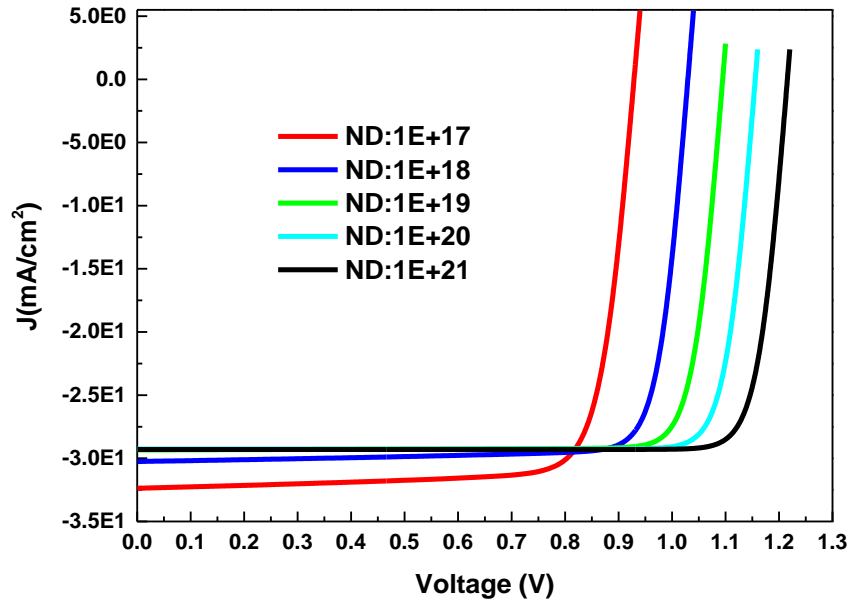


Figure 5. Acceptor density N_A ($1/\text{cm}^3$) effect on PCE.

Table 6. Varies acceptor density effect on V_{oc} , FF, J_{sc} , and PCE of the simulated FPSC at 300 K and 600 nm thickness.

| Density N_A ($1/\text{cm}^3$) | V_{oc} | J_{sc} | FF | Eta% |
|-----------------------------------|----------|-----------|-------|-------|
| 1E+17 | 0.9292 | 32.369757 | 80.31 | 24.15 |
| 1E+18 | 1.0299 | 30.252599 | 84.09 | 26.20 |
| 1E+19 | 1.0949 | 29.338074 | 86.78 | 27.87 |
| 1E+20 | 1.1558 | 29.271885 | 87.72 | 29.68 |
| 1E+21 | 1.2185 | 29.301536 | 88.07 | 31.44 |

Table 6 presents the optical values for flexible perovskite solar cells, organized based on the doping concentration ratios. The optimization of thickness was performed on a flexible perovskite solar cell at 300 K. As seen in figure 5 with doping concentrations of $1\text{E}+17$, $1\text{E}+18$, $1\text{E}+19$, $1\text{E}+20$, and $1\text{E}+21$, a thickness of 600 nm resulted in an efficiency value of 26.98%. Among these doping concentrations, the highest efficiency of 31.44% was achieved with a doping concentration of $1\text{E}+21$.

4. CONCLUSION

In this study, a simulation-based analysis was conducted on PET/ITO/ TiO_2 / $\text{CH}_3\text{NH}_3\text{SnI}_3$ /CuSCN/Ag flexible perovskite solar cells. The purpose of the analysis was to investigate the performance and characteristics of these specific solar cell configurations by using SCAPS 1D. In the optimization study of a flexible perovskite solar cell at 300 K, different doping concentrations were investigated for a fixed thickness of 600 nm. The resulting efficiency values showed that at this thickness, the cell achieved an efficiency of 26.98%. Among the tested doping concentrations, the highest efficiency of 31.44% was obtained with a doping concentration of $1\text{E}+21$.

SIMILARITY RATE: 15 %

CONFLICT of INTEREST

The authors declared that they have no known conflict of interest.

EXPLORING EFFICIENCY AND DESIGN OPTIMIZATION OF FLEXIBLE PEROVSKITE SOLAR CELLS USING SCAPS-1D SIMULATION

ACKNOWLEDGEMENT

The authors gratefully acknowledge Professor Marc Burgelman from the Department of Electronics and Information Systems at the University of Ghent for the development of the SCAPS software package and for granting permission to utilize it in this study.

REFERENCES

- [1] Kumar, Mulmudi Hemant, et al. "Flexible, low-temperature, solution processed ZnO-based perovskite solid state solar cells." *Chemical Communications* 49.94 (2013): 11089-11091.
- [2] Huang, Keqing, et al. "High-performance flexible perovskite solar cells via precise control of electron transport layer." *Advanced Energy Materials* 9.44 (2019): 1901419.
- [3] Xu, Zhiyuan, et al. "Functional layers of inverted flexible perovskite solar cells and effective technologies for device commercialization." *Small Structures* (2023): 2200338.
- [4] Docampo, Pablo, et al. "Efficient organometal trihalide perovskite planar-heterojunction solar cells on flexible polymer substrates." *Nature Communications* 4.1 (2013): 2761.
- [5] Di Giacomo, Francesco, et al. "Flexible perovskite photovoltaic modules and solar cells based on atomic layer deposited compact layers and UV-irradiated TiO₂ scaffolds on plastic substrates." *Advanced Energy Materials* 5.8 (2015): 1401808.
- [6] Heo, Jin Hyuck, et al. "Highly efficient low temperature solution processable planar type CH₃NH₃PbI₃ perovskite flexible solar cells." *Journal of Materials Chemistry A* 4.5 (2016): 1572-1578.
- [7] Lee, Eunsong, et al. "All-Solution-Processed Silver Nanowire Window Electrode-Based Flexible Perovskite Solar Cells Enabled with Amorphous Metal Oxide Protection." *Advanced Energy Materials* 8.9 (2018): 1702182.
- [8] Liu, Chang, et al. "Hydrothermally treated SnO₂ as the electron transport layer in high-efficiency flexible perovskite solar cells with a certificated efficiency of 17.3%." *Advanced Functional Materials* 29.47 (2019): 1807604.
- [9] Zhong, Meiyang, et al. "Highly efficient flexible MAPbI₃ solar cells with a fullerene derivative-modified SnO₂ layer as the electron transport layer." *Journal of Materials Chemistry A* 7.12 (2019): 6659-6664.
- [10] Qi, Jiabin, et al. "A kirigami-inspired island-chain design for wearable moistureproof perovskite solar cells with high stretchability and performance stability." *Nanoscale* 12.6 (2020): 3646-3656.
- [11] Cheng, Haiyang, et al. "KBF₄ Additive for Alleviating Microstrain, Improving Crystallinity, and Passivating Defects in Inverted Perovskite Solar Cells." *Advanced Functional Materials* 32.36 (2022): 2204880.
- [12] Han, Bin, et al. "Rational Design of Ferroelectric 2D Perovskite for Improving the Efficiency of Flexible Perovskite Solar Cells Over 23%." *Angewandte Chemie International Edition* 62.8 (2023): e202217526.
- [13] Marc. Burgelman, Department of Electronics and Information System, University of Gent. SCAPS-1D.
- [14] Anwar, Farhana, et al. "Effect of different HTM layers and electrical parameters on ZnO nanorod-based lead-free perovskite solar cell for high-efficiency performance." *International Journal of Photoenergy* 2017 (2017).
- [15] Hossain, M. Khalid, et al. "Effect of various electron and hole transport layers on the performance of CsPbI₃-based perovskite solar cells: A numerical investigation in DFT, SCAPS-1D, and wxAMPS frameworks." *ACS omega* 7.47 (2022): 43210-43230.
- [16] Hossain, M. Khalid, et al. "An extensive study on multiple ETL and HTL layers to design and simulation of high-performance lead-free CsSnCl₃-based perovskite solar cells." *Scientific Reports* 13.1 (2023): 2521.
- [17] Behrouznejad, Fatemeh, et al. "A study on utilizing different metals as the back contact of CH₃NH₃PbI₃ perovskite solar cells." *Journal of Materials chemistry A* 4.35 (2016): 13488-13498.
- [18] Goje, A. A., et al. "Design and Simulation of Lead-free Flexible Perovskite Solar cell Using SCAPS-1D." *IOP Conference Series: Materials Science and Engineering*. Vol. 1278. No. 1. IOP Publishing, 2023.
- [19] Slami, Abdelhadi, Mama Bouchaour, and Laarej Merad. "Numerical study of based perovskite solar cells by SCAPS-1D." *Int. J. Energy Environ* 3 (2019): 17-21.
- [20] Trukhanov, V. A., V. V. Bruevich, and D. Yu Paraschuk. "Effect of doping on performance of organic solar cells." *Physical Review B* 84.20 (2011): 205318.

